Ground-state phase diagram of Na_xCoO_2: correlation of Na ordering with CoO_2 stacking sequences

2009 J. Phys.: Condens. Matter 21 035401

(http://iopscience.iop.org/0953-8984/21/3/035401)

J. Phys.: Condens. Matter **21** (2009) 035401 (7pp) doi:10.1088/0953-8984/21/3/035401

Ground-state phase diagram of Na_xCoO_2: correlation of Na ordering with CoO_2 stacking sequences

Yanli Wang, Yi Ding and Jun Ni

Department of Physics and Key Laboratory of Atomic and Molecular Nanoscience (Ministry of Education), Tsinghua University, Beijing 100084, People's Republic of China

E-mail: junni@mail.tsinghua.edu.cn

Received 7 October 2008, in final form 21 November 2008
Published 11 December 2008
Online at stacks.iop.org/JPhysCM/21/035401

Abstract

We have proposed a Hamiltonian that takes into account both Na–Na interactions and coupling between Na ions and CoO_2 layers. By a combination of the Monte Carlo and first-principles approaches, all the possible stacking sequences of CoO_2 layers together with the Na ordering have been obtained. In particular, an infinite series of ground states of Na ordering has been predicted in P3-Na_xCoO_2. We have obtained the ground-state phase diagram with the variation of Na concentration, which explains well the complex variation of the CoO_2 stacking sequences. Our calculations show that the ordering of Na ions to minimize the Coulomb interaction is the main cause of the variation of the CoO_2 stacking sequences.

(Some figures in this article are in colour only in the electronic version)

1. Introduction

Since the superconductivity was discovered in the hydrated $Na_xCoO_2{\cdot}yH_2O$ at $x \sim 1/3$ [1], it has received extensive attention in recent years and creates an active area in the layered compound. Electronic and magnetic properties exhibit complex behavior as a function of Na concentration x [2, 3]. The Na_xCoO_2 compound is composed of layers of CoO_6 edge-sharing octahedra and Na layers intercalated between them. Different stacking sequences of CoO_2 layers result in a variety of host structures. There have been reported several types of structures in this layered compound, such as the O3-type, P2-type and P3-type structures [4]. In the designation, O or P describes the coordination geometry of Na ions and the number 2 or 3 indicates the number of CoO_2 layers in the unit cell.

Large progress has been made on P2-Na_xCoO_2, involving the unconventional magnetic and electronic properties [2, 5], as well as various Na-vacancy orderings [6–9]. The two-layered P2-type structure has been reported to exist in a large range of x in the unhydrated phase [7] and in the hydrated superconducting phase [1], while the three-layered crystal structure has been found to exhibit a complex behavior with the deintercalation of Na ions from O3-$NaCoO_2$ [10]. Experiments have reported that the variation of the stacking sequence is accompanied by the change of Na content x [4, 10]. However, the stability of various structures with the variation of Na concentration x remains unclear. Furthermore, there is no systematic investigation on the Na-vacancy ordering in the frame of the whole host structures and its relation to the stability of the stacking sequences. A systematic approach, considering both the Na ordering and the CoO_2 stacking sequences, is needed to clarify these issues.

In this work, we have proposed a Hamiltonian, which takes into account the Na–Na interaction and the coupling between Na and CoO_2 layers. Five types of structures in Na_xCoO_2 with different CoO_2 stacking sequences have been obtained, including O1-, O2-, O3-, P2- and P3-type structures. The ground-state phase diagram of the stacking structures with the variation of Na concentration x has been obtained and the stability of all the possible stacking structure types has been investigated. Our calculations are in good accordance with the experimental results. We have also predicted stable Na-vacancy ordering patterns in all these types of structures. In particular, an infinite series of ground states of Na ordering has been found in the P3-type structure.

2. Model and methods

In the layered system, CoO_2 sheets and Na layers alternate along the c axis. In each layer of Na, Co and O, the possible

sites for atoms to occupy form a lattice that can be divided into three triangular sublattices denoted by A, B and C. Figure 1 shows the schematic CoO_2 in-plane structure. We use σ_α^k = A(B, C) to represent a sublattice of the kth α (α = Na, Co, O) layer. In the Co and O layers, one sublattice is fully occupied leaving others empty [11]. For the CoO_2 sheet, the sublattices of Co and O layers are distinct, keeping the edge-shared CoO_6 octahedral configuration [4, 10]. There are two structural freedoms in the layered system, involving the Na ordering and the CoO_2 stacking sequences, which are coupled to each other. Since the interlayer distance of CoO_2 sheets is large [3, 8], we consider only the nearest-neighbor layer interaction between Na layers and CoO_2 sheets. We use the following Hamiltonian to describe the Na_xCoO_2 system:

$$H = \sum_k \sum_{\{\sigma_{\mathrm{Na}}^k, \sigma_{\mathrm{Na}}'^k\}} \sum_{\{i,j\}} J_{ij} n_i(\sigma_{\mathrm{Na}}^k) n_j(\sigma_{\mathrm{Na}}'^k) + \sum_{\{k,l\}} \sum_{\sigma_{\mathrm{Na}}^k} \sum_i (V_{\mathrm{Na-O}} \delta_{\sigma_{\mathrm{Na}}^k \sigma_{\mathrm{O}}^l} + V_{\mathrm{Na-Co}} \delta_{\sigma_{\mathrm{Na}}^k \sigma_{\mathrm{Co}}^l}) n_i(\sigma_{\mathrm{Na}}^k) + \sum_k \sum_{\sigma_{\mathrm{Na}}^k} \sum_i \mu n_i(\sigma_{\mathrm{Na}}^k) + V_1.$$

The first term is the interaction energy of Na ions within the Na plane described by the lattice gas model. The second term is the coupling term between Na ions and CoO_2 layers described by the Potts model. The third term is the chemical potential term of Na ions. The energy of CoO_2 layers has been included in the constant term V_1. In the first term, k runs over all the Na layers and $\{\sigma_{\mathrm{Na}}^k, \sigma_{\mathrm{Na}}'^k\}$ runs over all the three Na sublattices on the kth Na layer, where σ_{Na}^k and $\sigma_{\mathrm{Na}}'^k$ can take the values of A, B and C. $\{i, j\}$ runs over the neighboring sites on the sublattice σ_{Na}^k and $\sigma_{\mathrm{Na}}'^k$, respectively. J_{ij} is the pair interaction. The distance between the nearest neighbors of the two sublattices is 1.628 Å, while the radius of the Na ion is 1.02 Å. Thus, it is forbidden for Na ions to occupy nearest-neighbor sites in our model. We assign n_i $(\sigma_{\mathrm{Na}}^k) = 1(0)$ when the Na (vacancy) occupies site i on the sublattice σ_{Na}^k. In the second term, $\{k, l\}$ runs over the nearest-neighbor Na and CoO_2 layers, σ_{Na}^k runs over all three Na sublattices on the kth Na layer and i runs over all the Na sites within σ_{Na}^k. In the third term, k runs over all the Na layers, σ_{Na}^k runs over all the three Na sublattices on the kth Na layer and i runs over all the Na sites within σ_{Na}^k. μ is the chemical potential of Na ions. δ_{ij} is 1 when $i = j$, otherwise it is 0. When α ions and β ions face each other directly on the same type of sublattice, we call the interaction a direct one. When α ions and β ions are on different sublattices, we call the interaction an indirect one. The interaction parameter $V_{\alpha-\beta}$ represents the energy difference between direct and indirect interactions of α and β layers.

The combination of Monte Carlo (MC) simulations and first-principles methods have been used to search the ground-state structures [12–14]. First, the interaction parameters used in the MC simulations are determined from a series of energies of different structures calculated by the first-principles method. Then the MC simulated annealing is conducted to search all possible ground states. If new structures are obtained from the MC simulations, the energies of these structures are calculated by the first-principles calculations method, and the interaction parameters are recomputed with the energies of these structures

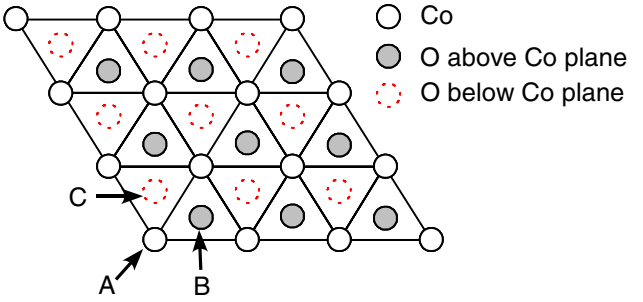

Figure 1. The in-plane structure for the CoO_2 layer. The white circles represent Co ions within the Co layer. The gray solid circles and dashed hollow circles denote the O ions above and below the Co layer, respectively. In a CoO_2 layer, the Co layer and two O layers occupy different triangular sublattices A, B and C.

incorporated. This procedure of MC simulations and first-principles calculations is continued until no new lower energy states are obtained. The stability of the ground states as a function of x is determined by comparing the total energies of these structures. The total energy calculations have been performed using VASP (the Vienna *ab initio* simulation package) [15]. The projector augmented wave [16] (PAW) method is used to describe the electron–ion interaction. In our calculations, the Perdew–Wang functional form [17] of the generalized gradient approximation (GGA) is adopted. The energy cutoff was set to be 500 eV. Supercells are relaxed because the lattice constant changes with the variation of x, especially in the c axis. All the atom coordinates are also fully relaxed. The tolerance of energy for the optimization is 10^{-4} eV. Brillouin zone integration was done with the origin at the Γ point. For large systems with more than 50 ions, a $3 \times 3 \times 2$ mesh is adopted and a $5 \times 5 \times 2$ k-mesh has been adopted for smaller systems in order to have the similar precision. To test the convergence with respect to the plane-wave cutoff and the k-point sampling, we repeated the calculations, increasing the k-mesh to $5 \times 5 \times 3$ for large systems and $7 \times 7 \times 5$ for small systems with cutoff energy of 800 eV. This did not change total energies by more than 3 meV/atom, which indicates that the chosen cutoff energy and k-points are sufficient for our calculated systems.

All the possible ground states of the system are obtained by simulated annealing which starts with a Metropolis Monte Carlo simulation at a high temperature in the grand canonical ensemble [18]. The system is annealed down from a state at high temperature to a state at low temperature to get the configuration with minimal free energy. When the temperature approaches zero, the system will be annealed into the ground state. In our MC simulations, we consider the nearest-neighbor interaction J_1 of Na ions on the same sublattice, the next-nearest-neighbor interaction J_2 on the same sublattice and the next-nearest-neighbor interaction J_{12} on different sublattices. The simultaneous occupancy of the nearest-neighbor sites on different sublattices is prohibited [8, 9]. From the first-principles calculations, the interaction parameters have been determined as $J_1 = 329.44$ meV, $J_2 = 4.04$ meV and $J_{12} = 119.16$ meV. The interaction parameter $V_{\mathrm{Na-O}}$ is determined to be 1.908 eV/Na. The value $V_{\mathrm{Na-O}}/J_1$ is so large that

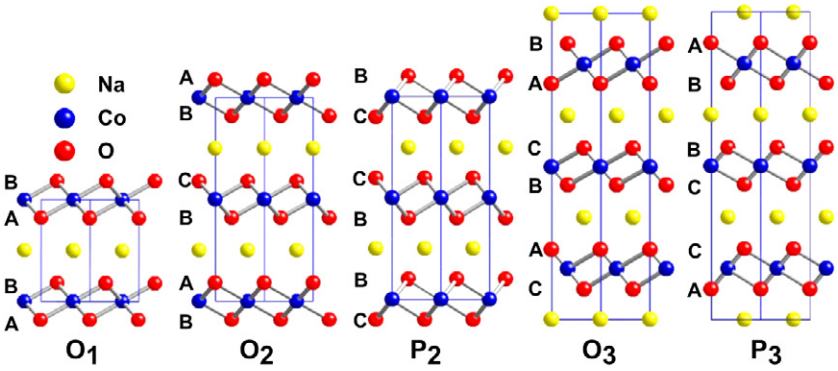

Figure 2. Schematic diagram of the five structures with different stacking sequences. The characters A, B and C denote the sublattices of O layers.

Na ions cannot occupy the same type of sublattice as that of adjacent O layers at both sides, which is in agreement with the experiment [19]. Therefore, with an O-type structure, for example ABC (O Na O), Na ions can only occupy one triangular sublattice (B), while for a P-type structure, for example A(B, C)A(O Na O), Na ions have two possibilities (B or C). The interaction parameter $V_{\mathrm{Na-Co}}$ serves as site energy of the Na sublattice. Our first-principles calculations give that $V_{\mathrm{Na-Co}} = 0.0863$ eV/Na. The interaction parameters are determined by mapping the formation energies of a series of optimized structures to the Hamiltonian. The formation energies of 22 P2-Na_xCoO_2 structures have been used, involving nine ground-state structures from $x = 0$ to 1, one structure at $x = 5/7$ from [7], four structures at $x = 3/4$ from [7, 20, 21], which have been believed to be stable, one structure at $x = 4/5$ from [9], two structures at $x = 2/3$ from [8] and five other structures with relatively high symmetry. These five structures include two structures at $x = 1/2$, one structure at $x = 7/9$, one structure at $x = 5/6$ and one structure at $x = 21/25$. To test the predictive power of these interaction parameters, we have compared the calculated formation energies using these parameters with the first-principles calculated values of other stacking structures (including 11 P3-, 7 O1-, 7 O2- and 7 O3-type structures with various Na content x). Our calculations show that the energy differences are small, which demonstrates that these interaction parameters are effective for structures with different CoO_2 stacking sequences and that the truncation of the interaction parameters are sufficient. Moreover, using these interaction parameters, the ground Na orderings for the five types of stacking structures from MC simulations are in good accordance with the first-principles results. Although some of these interaction parameters are only a few meV, which is comparable with the density function theory accuracy in the total energy calculations, it should be noted that the interaction parameters are more influenced by the truncation of the interactions and the configurations used in the determination of these interaction parameters [22, 23]. Both the good predictive power of these interaction parameters and the good accordance between the MC results and first-principles results imply the reliability of these interaction parameters.

3. Results

For the one-dimensional lattice with the nearest-neighbor interaction only, the ground state structures can be constructed by the local configurations with minimum energy [24]. From our Hamiltonian with the coupling between Na layer and adjacent CoO_2 layers, there are five stacking configurations: O1-, O2-, O3-, P2- and P3-Na_xCoO_2, as shown in figure 2.

3.1. Na ordering in O-type Na_xCoO_2

In the O-type stacking sequences, Na ions can occupy the sites of only one triangular sublattice and each Na layer has the octahedral coordination formed by different sublattices of the adjacent O layers. When the nearest interaction J_1 and the next-nearest-neighboring interaction J_2 are considered, there are nine possible ground-state structures on a planar triangular lattice [25, 26]. Our first-principles calculations show that the seven stable Na patterns at $x = 1/4$, $1/3$, $1/2$, $2/3$, $3/4$ and 1 are ground states, which are shown in figure 3(a). With the energies of these ground-state structures calculated from first principles, the parameters J_1 and J_2 can be determined using the regression method. Our calculations show that the differences of the energy parameters J_1 and J_2 between different stacking structures are small. For example, for O2-Na_xCoO_2, $J_1 = 363.6$ meV and $J_2 = 10.32$ meV, while $J_1 = 329.44$ meV and $J_2 = 4.04$ meV for P2-Na_xCoO_2. The small difference between the two cases suggests that the Na–Na in-plane interactions are not sensitive to the stacking sequence of CoO_2 layers. This is quite reasonable, considering that the distance between CoO_2 layers is large. Using these parameters, the Na ordering structures can be determined from Monte Carlo simulations and they are in good accordance with the first-principles calculations. All these Na ordering structures are common on the triangular lattice, which also exist in Li_xCoO_2 with Li–Li repulsion as the main factor for ordering [27].

3.2. Na ordering in P-type Na_xCoO_2

In the P-type structures, the two neighboring O layers of the Na layer face each other directly, which provides the prismatic coordination for Na ions. Instead of a single triangular lattice

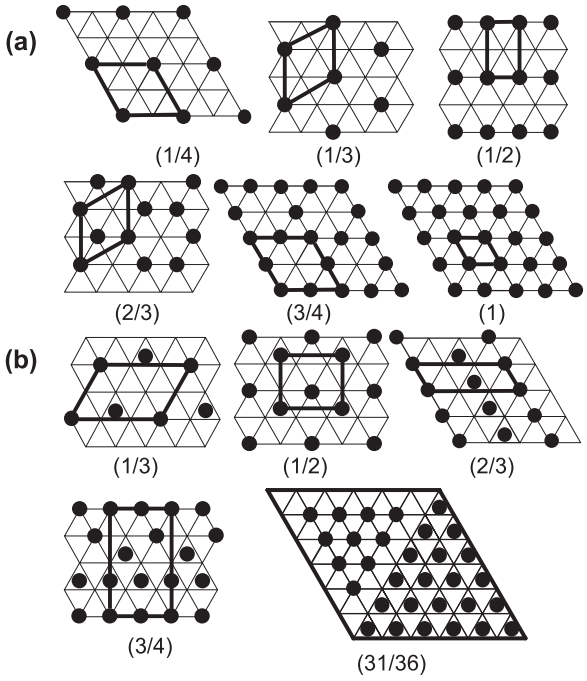

Figure 3. Ordered structures of Na ions (a) in the O-type structures. The triangular lattice denotes Na sites within the Na plane. (b) In the P3-type structure. The triangular lattice is for the Na1 site and the centers of the triangles are for Na2 sites. Solid black circles represent the sites occupied by Na ions.

for the Na sites in the O-type stacking sequences, there are two intervening triangular sublattices for Na sites in the P2-, P3-Na_xCoO_2, namely Na1 and Na2. In the P2-type structure, Na1 sites have larger site energy than Na2 sites due to the direct repulsion between Na and adjacent Co ions, while in the P3-type structure, Na1 and Na2 sites are equivalent. In our previous study, the Na ordered structures of P2-Na_xCoO_2 have been obtained with a combination of Monte Carlo and first-principles approach [8]. Using the same method we have obtained the Na ordering structures in P3-Na_xCoO_2. The same Na ion interaction parameters have been adopted by considering that these parameters are not sensitive to the stacking sequence of CoO_2 layers, as shown in section 3.1. The first-principles calculations are in good accordance with the Monte Carlo results. For $x \leqslant 31/36$, the stable Na ordering patterns are predicted at $x = 1/3$, $1/2$, $2/3$, $3/4$ and $31/36$, as shown in figure 3(b). The details about the infinite series of Na ordering patterns are discussed in section 3.3.

At $x = 1/3$, different from the $\sqrt{3}\times\sqrt{3}$ superstructure for P2-$Na_{1/3}CoO_2$, the ground-state structure of P3-$Na_{1/3}CoO_2$ corresponds to a 2×3 rhombic lattice with equal occupancy on Na1 and Na2 sites, as shown in figure 3(b). This is due to the fact that Na1 and Na2 sites are equivalent in the P3-type structure, while in the P2-type structure there exist energy differences between Na1 and Na2 sites and Na ions occupy Na2 sites only at low concentrations. The difference indicates that CoO_2 stacking sequences have great influence on the Na ordering.

At $x = 1/2$, Na ions arrange themselves in a $2 \times \sqrt{3}$ zigzag pattern, the same as P2-$Na_{1/2}CoO_2$. This arrangement agrees well with the experimental results [10, 28]. With this ordering pattern, a similar charge ordering picture in CoO_2 can be expected as that observed in P2-Na_xCoO_2. Phase transitions at low temperature have also been reported in P3-$Na_{1/2}CoO_2$, very similar to P2-Na_xCoO_2 [10]. With the same trigonal prismatic coordination, P2- and P3-Na_xCoO_2 share many common features.

At $x = 2/3$, a 3×1 rhombic superstructure has been predicted as a ground-state structure with alternating rows of Na ions on Na1 and Na2 sites.

We find a ground state at $x = 3/4$ with a $2\sqrt{3} \times 2$ orthogonal superstructure as shown in figure 3(b). This ordering pattern coincides with that observed by neutron diffraction experiment for γ-$Na_{0.75}CoO_2$ [29]. Due to the special Na arrangement of P3-$Na_{0.75}CoO_2$, stripelike charge correlations will be expected as proposed by Geck *et al* [29]. The superstructure at $x = 31/36$ corresponds to the 6×6 rhombic superlattice, as shown in figure 3(b).

3.3. Infinite series of ground states of Na ions in P3-Na_xCoO_2

For $x > 31/36$, we find an infinite series of ground states at high Na concentration range from MC simulations. These ground-state structures have M-vacancy patterning, but with a slightly different arrangement from those in [9]. At high concentrations, MC results show that M vacancies arrange themselves as far away as possible to minimize the repulsion interaction energy. At and above a critical concentration, which corresponds to the most close-packed M-vacancy patterns that are independent of each other, the Hamiltonian of the system can be expressed analytically:

$$H = C_1 + \left(C_2 + \frac{C_3}{M}\right)(1 - x) + x\mu$$

where $C_1 = 3J_1 + 3J_2$, $C_2 = -9J_1 + 3J_{12} - 15J_2$, $C_3 = 3J_1 - 3J_{12} + 12J_2$. For close-packed M vacancies without interactions with $x = x_{\min}$, there are two types of close-packing M-vacancy structures. The first pattern is a $(M + 1) \times (M + 1)$ rhombic superlattice and the corresponding Na concentration is $x_1 = 1 - M/(M + 1)^2$. In the second pattern, M vacancies arrange themselves in such a way that each apex of the M vacancy points to the edge center of other M-vacancy triangles. The corresponding Na concentration is $x_2 = 1 - 4M/(3M^2 + 12M + A)$ ($A = 12$ for an even number M and $A = 13$ for an odd number M). With $x_{\min} = \min(x_1, x_2)$, we can obtain that, for $M \leqslant 5$, the ground-state structure corresponds to the first pattern and for $M > 5$ the ground-state structure corresponds to the second pattern. The number M of the ground-state structure can be determined using the formula $\mathrm{d}(H(M))/\mathrm{d}M = 0$. When $M \leqslant 5$, the number $M = (\mu - C_2 + 2C_3)/(\mu - C_2)$; when $M > 5$, the number $M = [3C_3 + \sqrt{9C_3^2 + 3(\mu - C_2)(A\mu - AC_2 + 13C_3)}]/3(\mu - C_2)$. As an integer, M is determined by comparing the Hamiltonian of $H(M_z + 1)$ and $H(M_z)$, where M_z is the integral part of M. From the above expression, we can see that, when μ approaches C_2, M grows to infinity. The shape of the M vacancy is somewhat similar to the T series of the three infinite series of ground states in the hexagonal

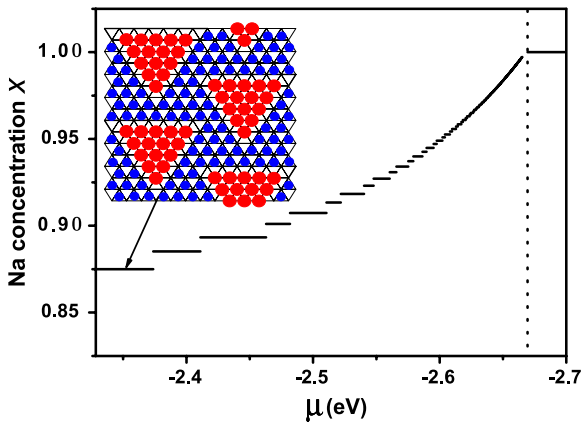

Figure 4. Na concentration x of the infinite series of ground states of Na ions in P3-Na_xCoO_2 as a function of the chemical potential μ. The inset shows the M-vacancy patterns for $M = 6$. Large (red) and small (blue) circles represent atom occupancy at Na1 and Na2 sites, respectively. The dashed line indicates the critical chemical potential.

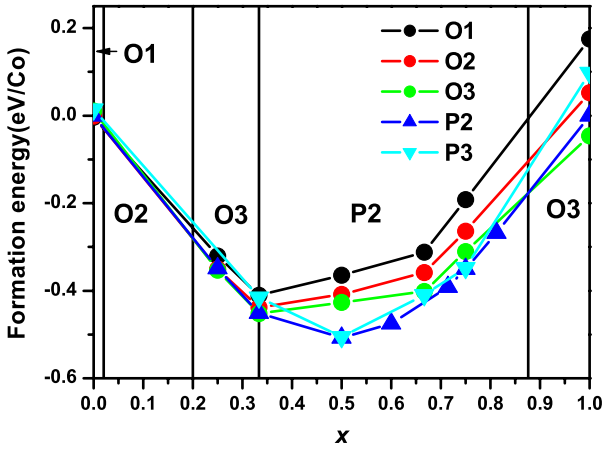

Figure 5. The ground-state phase diagram and formation energies of the ground-state structure in Na_xCoO_2 as a function of x. The phase name between the phase boundaries denotes the stable phase in the region.

lattice [30]. But this infinite series of ground states is different from that in the hexagonal lattice [30] due to the fact that the nearest-neighboring sites on the two intervening triangular sublattices cannot be occupied simultaneously in the Na_xCoO_2 system. With the increase of M, Na concentration x increases accordingly. Figure 4 illustrates the Na concentration x with the variation of chemical potential. At the limitation $x = 1$, only one sublattice is completely occupied, leaving the other empty. In the high Na concentration region, the most stable stacking sequence is O3-Na_xCoO_2. This infinite series of ground states is not stable globally when the stacking sequence is considered. This explains why this infinite series of ground states has not been observed in experiments so far. However, if one keep the P3-type structure when increasing the concentration of Na ions, one can observe this infinite series of Na ordering.

3.4. Ground-state phase diagram of Na_xCoO_2 with different stacking sequences

After determining the ordered patterns of sodium ions in each type of structures, we are able to obtain the ground states of Na_xCoO_2 as a function of x by comparing the total energies of these structures. After the optimization, our calculations show that the in-plane lattice constant undergoes only slight expansion with the increase of x, while the lattice constant in the c axis shrinks with the increase of x. This result is in good accordance with the experimental results [10]. In addition, the optimized structures agree well with the experiments. In the case of CoO_2, our calculations show that, for O1-CoO_2, $a = 2.81$ Å and $c = 4.29$ Å, which is in good accordance with the experimental result that $a = 2.82$ Å and $c = 4.23$ Å [31]. Figure 5 displays the formation energies of the stable Na ordering patterns in all the stacking structures. The formation energy is defined as: $E_b(\sigma) = E_x(\sigma) - xE_{P2-NaCoO_2} - (1-x)E_{P2-CoO_2}$. Here, $E_x(\sigma)$ is the total energy of structure σ at x, and $E_{P2-NaCoO_2}$ and E_{P2-CoO_2} are the energies of P2-$NaCoO_2$ and P2-CoO_2, respectively. With this definition, we can deduce that, at each concentration x, the formation energy difference between structures equals their total energy difference. Thus the most stable stacking sequence at a certain x is the one with the lowest formation energy. The phase boundary of two host structures corresponds to the crossing point of the formation energy curves of the two structures. From this figure, we can see that the ground-state structures of Na_xCoO_2 changes in a complex way with the variation of x. The general tendency is that the O-type structures are preferred at low doping level $x < 1/3$ and high doping $0.876 < x \leqslant 1$, while in the intermediate range the P-type structures, which have prismatic coordination for the Na ions, become more stable. The Na concentration x plays an essential role in tuning the stacking sequence of CoO_2, which we will discuss in detail below.

In the small range of $0 \leqslant x < 0.02$, O1-Na_xCoO_2 is the most stable one, which is in good agreement with the experiments [31, 32]. However, E_b of O2- and P2-CoO_2 are only 2.8 meV/Co and 3.59 meV/Co higher than O1-CoO_2, respectively. The small energy differences indicate that they can be considered as degenerate structures. O3- and P3-CoO_2 are less preferable, whose formation energies are 14.41 and 18.49 meV/Co higher than that of O1-CoO_2, respectively. This is in agreement with the experiment that P3-CoO_2 is metastable [32]. At low concentration range $0.02 < x \leqslant 0.20$, O2-Na_xCoO_2 becomes the most stable one. O2-, O3- and P2-Na_xCoO_2 are almost degenerate in energy, while O1- and P3-Na_xCoO_2 are unfavorable structures. In the range of $0.2 < x \leqslant 0.336$, O3-Na_xCoO_2 is the most stable structure. At $x = 1/3$, P2-Na_xCoO_2 is only 1.5 meV/Co higher in energy than O3-Na_xCoO_2 and they can be considered as degenerate structures. The other three structures have much higher formation energies than O3-Na_xCoO_2.

In the range of $0.336 < x < 0.876$, the P2-type structure becomes the most preferable structure. P2-Na_xCoO_2 has been successfully synthesized in this range of x [7, 9]. At $x = 1/2$, P3-$Na_{1/2}CoO_2$ is only 1.84 meV/Co higher in energy than P2-$Na_{1/2}CoO_2$, while the O-type structures are unstable

with much higher formation energies. At $x = 2/3$, P2-Na_xCoO_2 will undergo a phase separation into the structures of $x = 3/5$ and $5/7$ [8]. P3-$Na_{2/3}CoO_2$ is 17.06 meV/Co higher than the phase separation energy. The small energy difference means that P3-$Na_{2/3}CoO_2$ may exist as a metastable structure. Actually, Ong *et al* have reported to have synthesized the crystal structure of P3-$Na_{0.67}CoO_2$ [33]. For $x = 3/4$, our calculations show that the ground state is P2-Na_xCoO_2, which agrees with the experiments [4, 7, 29]. P3-Na_xCoO_2 is only 2.66 meV/Co higher in energy than P2-Na_xCoO_2 and they can be viewed as degenerate structures. At $x = 3/4$, a distorted monoclinic structure has been synthesized in experiments [4, 10]. Since the space group of the monoclinic structure observed in experiments is $C2/m$ [4, 10], which is the same as that of the P3-type structure with small distortions [33], we speculate that it is the P3-type structure with small distortions. However, within the accuracy of our calculations, we have not obtained such distortions in the O3 or P3 phase. The reason that the P-type structures are more stable than the O-type structures can be explained as follows: the Na–Na Coulomb interaction is the main factor for Na ordering. With the increase of Na ions, the Coulomb interactions of Na ions in the O-type structures increase rapidly because only one triangular sublattice can be occupied by Na ions, while in the P-type structures there are two intervening sublattices with more sites for Na ions to occupy, which can effectively reduce the interactions.

At high concentration $0.876 < x \leqslant 1$, most of the Na ions occupy one sublattice. As a result, for the P-type structures, the energy gain from the partial occupancy of the two sublattices decreases with the increase of x. The energy differences between different structures come mainly from the coupling between the Na layer and CoO_2 layers. Thus O3-Na_xCoO_2 becomes the most stable structure at high concentration x, which is in agreement with the experimental result [4].

As we know, the ground-state structure involves both the CoO_2 stacking sequence and the Na ordering. Figure 5 shows a succession of O1, O2, O3, P2 and O3 phases with different stacking sequences for the ground-state structure as a function of x. With respect to the Na ordering at x, it is either a homogeneous superstructure or a phase separation within the frame of the CoO_2 stacking sequence.

4. Discussion

The stacking sequences can be transformed into each other by gliding CoO_2 sheets or by rearrangement within the CoO_2 layers. The rearrangement of CoO_2 layers involves breaking the Co–O bonds and is prevented by high barrier energy [11]. However, the gliding of CoO_2 sheets involves only a low barrier energy without breaking the Co–O chemical bonds [32]. The gliding of the CoO_2 sheets is usually realized via the soft chemical treatment using various agents such as HCl, Cl_2, I_2, etc. The gliding mechanism has been associated with the formation of nucleation centers and structural defects [34]. The five stacking structures can be divided into two groups: the first group with O1-, O3- and P3-Na_xCoO_2, and the second group with O2- and P2-Na_xCoO_2. In each group, the structures can be transformed into others through a proper gliding. But it is difficult to transform the structures in different groups into each other due to the requirement of breaking the Co–O bonds [11, 32].

The procedure of deintercalation of Na ions with soft chemical treatment can be used for the structural transformations through gliding. Our results provide a picture for such structural transformations with the change of x. Comparing the relative stabilities of the structures in the first group, O3-Na_xCoO_2 is the most stable structure in the high concentration range $0.8 < x < 1$, while in the range of $0.386 < x < 0.80$, P3-Na_xCoO_2 becomes the most stable structure with effective reduction of Na–Na interactions. This is in good accordance with the experiments. With the deintercalation of Na ions from O3-$NaCoO_2$, P3-Na_xCoO_2 of various concentrations has been successfully synthesized in this concentration range [10, 28, 35]. For $0.08 < x \leqslant 0.386$, O3-Na_xCoO_2 becomes the most stable structure again, which explains why O3-Na_xCoO_2 has been obtained at $x = 0.31$ instead of the P3-type structure in experiments [10]. In all the five types of structures, only O2-Na_xCoO_2 has not been reported in experiments. In the second group, the O2-type structure is more stable than the P2-type structure in the range of $0 < x < 0.25$, which suggests that O2-Na_xCoO_2 can be synthesized from P2-Na_xCoO_2 using soft chemical treatment in this range of x.

As the alkali cobalt oxides, Li_xCoO_2 and Na_xCoO_2 share similarities in many aspects. However, there are still differences between them. With respect to the structural properties, there are O3, O2, P3 and O1 phases existing in Li_xCoO_2 [36]. But the P2-type structure has not been reported yet in Li_xCoO_2, which is a common structure in Na_xCoO_2. Ion exchange reaction leads to O2-Li_xCoO_2 instead of the P2 phase [37]. We have shown that the change of the stacking sequence in Na_xCoO_2 is mainly caused by the ordering of Na ions to minimize the Na–Na interactions. In the Ising model, the nearest-neighbor interaction for Na ions is $J_1 = 82.36$ meV from our calculations [8], while for Li–Li interactions $J_1 = 29$ meV [38]. According to the correspondence between the Ising model and lattice gas model [39], J_1 for the Na–Na interaction is 329.44 meV in the lattice gas model, which is four times that in the Ising model. The nearest-neighbor interaction between Li ions is much smaller than that between Na ions, which means that the screening effect is stronger for Li ions in the Li_xCoO_2 system. Since the distance between CoO_2 in Li_xCoO_2 layers is smaller than that in Na_xCoO_2 due to the smaller radius of Li ions, Li ions are screened more strongly by the surrounding O ions with negative charges. The smaller effective positive charges of Li ions makes the Coulomb interaction much weaker between Li ions than that between Na ions. The energy gain through transformation from the O-type to P2-type structure due to the possibility of rearrangement of alkali ions is much smaller in the Li_xCoO_2 system than in Na_xCoO_2. In addition, the energy cost due to the direct repulsion between CoO_2 layers in the P2-type structure is larger in the Li_xCoO_2 system because Li_xCoO_2 has a smaller CoO_2 distance than Na_xCoO_2. The two factors make the O2-type structure more preferable in Li_xCoO_2 while the P2-type

structure is stable in Na_xCoO_2 in the intermediate range of x. This explains well that P2-Na_xCoO_2 transforms into O2-Li_xCoO_2 by ion exchange reaction in the experiment [37].

It should be mentioned that, in our investigation of the ground-state structures of Na_xCoO_2, the total energy calculations give only stability at zero temperature. The finite-temperature effects, such as the vibrational entropy and disorder-associated configuration entropy, have not been taken into account.

5. Conclusion

In conclusion, we have proposed a Hamiltonian to investigate the stable structures of Na_xCoO_2 as a function of x. Five structure types together with the Na ordering in each structural type have been obtained. We have predicted that O2-Na_xCoO_2 is a stable structure in the range of $0.02 < x < 0.20$ and an infinite series of ground states of Na ordering exists in P3-Na_xCoO_2. The ground-state phase diagram with the variation of Na concentration x has been obtained, which explains well the experimental results. Our calculations show that the change of the stacking sequence of CoO_2 layers is mainly caused by the Na ordering. In addition, comparison has been made between Li_xCoO_2 and Na_xCoO_2. In Li_xCoO_2, the most common structure is the O2 phase instead of the P2 phase, while the P2 phase is a common structural type in Na_xCoO_2. The reason is attributed to the Coulomb interaction of Na ions in Na_xCoO_2. Our previous study has concentrated on the Na-vacancy ordering in γ-Na_xCoO_2 with the P2-type structure [8]. In this work, we investigate both the Na ordering and the CoO_2 stacking sequence of the Na_xCoO_2 system. We find strong coupling between the two structural degrees of the compound. The CoO_2 stacking sequence determines the sublattice for Na ions to occupy and the Na ordering in turn is the driving force for the change in the CoO_2 stacking sequence.

Acknowledgments

This research was supported by the National Science Foundation of China (nos. 10674076 and 10721404) and MOST (2006CB605105).

References

[1] Takada K, Sakurai H, Takayama-Muromachi E, Izumi F, Dilanian R A and Sasaki T 2003 *Nature* **422** 53
[2] Foo M L, Wang Y Y, Watauchi S, Zandbergen H W, He T, Cava R J and Ong N P 2004 *Phys. Rev. Lett.* **92** 247001
[3] Zhang P H, Luo W D, Crespi V H, Cohen M L and Louie S G 2004 *Phys. Rev.* B **70** 085108
[4] Fouassier C, Matejka G, Reau J M and Hagenmuller P 1973 *J. Solid State Chem.* **6** 532
[5] Luo J L, Wang N L, Liu G T, Wu D, Jing X N, Hu F and Xiang T 2004 *Phys. Rev. Lett.* **93** 187203
[6] Huang Q, Foo M L, Lynn J W, Zandbergen H W, Lawes G, Wang Y Y, Toby B H, Ramirez A P, Ong N P and Cava R J 2004 *J. Phys.: Condens. Matter* **16** 5803
[7] Zandbergen H W, Foo M L, Xu Q, Kumar V and Cava R J 2004 *Phys. Rev.* B **70** 024101
[8] Wang Y L and Ni J 2007 *Phys. Rev.* B **76** 094101
[9] Roger M, Morris D J P, Tennant D A, Gutmann M J, Goff J P, Hoffmann J-U, Feyerherm R, Dudzik E, Prabhakaran D, Boothroyd A T, Shannon N, Lake B and Deen P P 2007 *Nature* **445** 631
[10] Viciu L, Bos J W G, Zandbergen H W, Huang Q, Foo M L, Ishiwata S, Ramirez A P, Lee M, Ong N P and Cava R J 2006 *Phys. Rev.* B **73** 174104
[11] Takada K, Sakurai H, Muromachi E T, Izumi F, Dilanian R A and Sasaki T 2004 *Adv. Mater.* **16** 1901
[12] Barabash S V, Blum V, Müller S and Zunger A 2006 *Phys. Rev.* B **74** 035108
[13] Osorio-Guillsén J, Zhao Y J, Barabash S V and Zunger A 2006 *Phys. Rev.* B **74** 035305
[14] Ceder G 1998 *Curr. Opin. Solid State Mater. Sci.* **3** 533
[15] Kresse G and Furthmuller J 1996 *Comput. Mater. Sci.* **6** 15
Kresse G and Furthmuller J 1996 *Phys. Rev.* B **54** 11169
[16] Blochl P E 1994 *Phys. Rev.* B **50** 17953
Kresse G and Joubert D 1999 *Phys. Rev.* B **59** 1758
[17] Perdew J P, Chevary J A, Vosko S H, Jackson K A, Pederson M R, Singh D J and Fiolhais C 1992 *Phys. Rev.* B **46** 6671
[18] Newman M E J and Barkema G T 1999 *Monte Carlo Methods in Statistical Physics* (Oxford: Oxford University Press)
[19] Balsys R J and Davis R L 1996 *Solid State Ion.* **93** 279
[20] Geck J, Zimmermann M v, Berger H, Borisenko S V, Eschrig H, Koepernik K, Knupfer M and Büchner B 2006 *Phys. Rev. Lett.* **97** 106403
[21] Meng Y S, Van der Ven A, Chan M K Y and Ceder G 2005 *Phys. Rev.* B **72** 172103
[22] Zarkevich N A and Johnson D D 2004 *Phys. Rev. Lett.* **92** 255702
[23] Blum V and Zunger A 2004 *Phys. Rev.* B **70** 155108
[24] Karl G 1973 *Phys. Rev.* B **7** 2050
[25] Yang X B and Ni J 2003 *Phys. Rev.* B **67** 195403
[26] Kudō T and Katsura S 1976 *Prog. Theor. Phys.* **56** 435
[27] Ceder G and Van der Ven A 1999 *Electrochim. Acta* **45** 131
[28] Yang H X, Xia Y, Shi Y G, Tian H F, Xiao R J, Liu X, Liu Y L and Li J Q 2006 *Phys. Rev.* B **74** 094301
[29] Geck J, Zimmermann M v, Berger H, Borisenko S V, Eschrig H, Koepernik K, Knupfer M and Büchner B 2006 *Phys. Rev. Lett.* **97** 106403
[30] Kanamori J 1984 *J. Phys. Soc. Japan* **53** 250
[31] Motohashi T, Katsumata Y, Ono T, Kanno R, Karppinen M and Yamauchi H 2007 *Chem. Mater.* **19** 5063
[32] Venkatraman S and Manthiram A 2002 *Chem. Mater.* **14** 3907
[33] Ono Y, Ishikawa R, Miyazaki Y, Ishii Y, Morii Y and Kajitani T 2002 *J. Solid State Chem.* **166** 178
[34] Tournadre F, Croguennec L, Saadoune I, Carlier D, Shao-Horn Y, Willmann P and Delmas C 2004 *J. Solid State Chem.* **177** 2790
Tournadre F, Croguennec L, Saadoune I, Carlier D, Shao-Horn Y, Willmann P and Delmas C 2004 *J. Solid State Chem.* **177** 2803
[35] Takada K, Osada M, Izumi F, Sakurai H, Takayama-Muromachi E and Sasaki T 2005 *Chem. Mater.* **17** 2034
[36] Wang M J, Navrotsky A, Venkatraman S and Manthiram A 2005 *J. Electrochem. Soc.* **152** 82
[37] Carlier D, Saadoune I, Croguennec L, Menetrier M, Suard E and Delmas C 2001 *Solid State Ion.* **144** 263
[38] Van der Ven A, Aydinol M K, Ceder G, Kresse G and Hafner J 1998 *Phys. Rev.* B **58** 2975
[39] Pathria R K 1996 *Statistical Mechanics* 2nd edn (Oxford: Butterworth–Heinemann) p 320